



GeoVirtual
2020 September
14-16
Resilience and Innovation



Estimation of pore fluid pH effect on Skempton's pore pressure parameter B_w

Debnath Mondal, Debasis Roy & Saswati Ghatak

Department of Civil Engineering – Indian Institute of Technology Kharagpur, Kharagpur, West Bengal, India

ABSTRACT

Since near-surface aerobic biologic processes produce CO_2 , the amount of biogenic CO_2 is expected to influence pore fluid compressibility. Consequently, pore water pressure development during events that deform a soil mass that holds microorganisms that produce CO_2 rapidly is also expected to depend on CO_2 production, as will be the liquefaction susceptibility of such soils. However, bacterial metabolic processes, life cycle, and CO_2 production affect pore fluid pH as well. That, in turn, would affect CO_2 solubility. The relationship between Skempton's pore water pressure parameter, B_w – the ratio of pore water pressure rise during rapid deformation of soil mass to the corresponding incremental mean normal stress – and the amount of CO_2 production is expected to be pH-dependent. A pH-dependent relationship between B_w and CO_2 amount has been derived here from theoretical considerations. The relationship was validated against the data from a series of closed-system laboratory experiments on loose sand that hosted two species of aerobic soil bacteria, *Lysinibacillus* sp. (DRG3) and *Bacillus megaterium* (RB-05). These species were minimally sustained within pore space in such a manner that one of three distinct metabolic pathways was triggered; one involving the production of exocellular metabolic substances (EPS), while the other two involving the production of EPS and calcite in the presence and absence of urea. Amounts of CO_2 , pH, and the corresponding values of B_w were tracked over up to 72 hours for these cases. B_w estimates from the theoretical relationship derived herein were found to agree reasonably with experimentally obtained values.

RÉSUMÉ

Puisque les processus biologiques aérobies en surface peuvent produire du CO_2 , on s'attend à ce que la quantité de CO_2 biogénique influence la compressibilité des fluides poreux. Par conséquent, le développement de la pression de l'eau des pores lors d'événements qui déforment une masse de sol qui contient rapidement des micro-organismes qui produisent rapidement du CO_2 devrait dépendre de la production de CO_2 , tout comme la susceptibilité à la liquéfaction de ces sols. Cependant, les processus métaboliques bactériens, le cycle de vie et la production de CO_2 affectent également le pH des fluides pores. Cela affecterait à son tour la solubilité du CO_2 . La relation entre le paramètre de pression de l'eau des pores de Skempton, B_w – le rapport de l'augmentation de la pression de l'eau des pores lors de la déformation rapide de la masse du sol au stress normal moyen progressif correspondant – et la quantité de production de CO_2 devrait être dépendante du pH. Une relation dépendante du pH entre la quantité de B_w et de CO_2 a été dérivée ici de considérations théoriques. La relation a été validée par rapport aux données d'une série d'expériences de laboratoire à système fermé.

1 INTRODUCTION

Biogenic gas produces from biological activities of microorganisms within the soil matrix at specific nutrient availability into the pore fluid. Such microbial activities lead to the production of bio-minerals like exo-cellular metabolic substances (EPS) and calcite (CaCO_3) (Ghatak 2017). Generally, near-surface aerobic biological processes produce CO_2 , H_2 , CH_4 , and N_2 . The biogenic carbon dioxide (CO_2) has high solubility resulting in low residency time within pore space (Rebata-Landa et al. 2012). The CO_2 partly dissolved in

the pore medium and remaining exists as a continuous phase, or occluded gas bubbles that significantly increases the compressibility of pore fluid, thus affect the degree of saturation indicated by Skempton's pore pressure parameter B_w . As a result, dissipating pore water pressure during cyclic loading reduces the liquefaction susceptibility of granular soil deposit. The amount of dissolved CO_2 decreases the pH through biogeochemical reactions and affects the solubility of the aqueous solution at a specific temperature and pressure. Bacteria inoculated soil sample retains more CO_2 at a pH level of 8.0; a lower microbial growth

results at pH level 6.0 (ASTM D5988-12). Hence at a low pH level free gas bubble generated at the surface and affects the saturation and compressibility of than high pH level. So it can be established that the solubility of nutrient pore fluid depends on the composition of bio-minerals (i.e., calcite, EPS), physical (i.e., temperature, pressure) and chemical (pH) characteristics. This study presents an investigation on the pH effect of pore fluids on solubility and saturation ratio in terms of Skempton's pore pressure parameter B_w through an analytical model, which shows an excellent agreement with experimental observation.

2 LITERATURE REVIEW

Microbial activities within the pore space generate biogases that exist along with the dissolved and free form. Isolated free or occluded gas bubbles significantly increase the pore fluid compressibility than dissolved gases (Ghatak et al. 2017). Occlude gas bubbles are not in contact with the mineral surfaces. Biogenic Nitrogen gas has low solubility and high residency time in the pore medium. As a result, it decreases the bulk stiffness of pore fluid and Skempton's B_w parameter (Rebata-Landa et al. 2012). The partially saturated uerolytic microbial calcium precipitated sand sample is more reliable than a fully saturated sand sample at identical calcite levels (Cheng et al. 2013). Anaerobic bacterial activities produce methane, which also significantly affects pore fluid compressibility but has a low effect on the undrained shear strength of fine-grained soils (Sills et al. 1991).

3 MATERIAL AND METHODS

3.1 Sand

Soil grain size has significantly affected the early evolution of bio-mediated gas generation. A poorly graded (SP) subangular siliceous sand (97% Quartz, ~3% feldspar) compatible with microbial activities was used in this research, having median particle size (D_{50}) of 0.55 mm, uniformity coefficient (C_u) of 1.99, maximum and minimum void ratio of 0.83 and 0.54 respectively, specific gravity (G_s) of 2.65. The sand was washed through 0.25 (N) HCl and 0.25 (N) NaOH successively and neutralized (pH 7.0) by distilled water. The washed moist sand was dried at 105°C and sterilizing by autoclaving at 121°C with 100 kPa for 15 minutes to avoid the contamination from the aerobic microorganism.

3.2 Microorganisms and Metabolic Pathways

Two endemic species soil bacterial strain *Lysinibacillus sp.* (DRG3) and *Bacillus megaterium* (RB-05) used to host live bacterial population within sand samples saturated with a nutrient medium for three distinct, minimally sustained metabolic processes (Table 1). Metabolic pathways abbreviated as per the nutrient medium characteristics and microbial products. Biological activities optimized at 35°C at the bacterial

strain rate of 6 g/L within the loose saturated sand model under elevated nutrient medium.

Table 1. Metabolic Pathways for bacterial strains

Metabolic Pathways	Bacterial Strain	Medium Characteristics
EPS ¹	DRG3, RB-05	No CaCl ₂ and Urea (CO(NH ₂) ₂)
NU ²	DRG3	CaCl ₂ (Ca ²⁺)
U ³	DRG3, RB-05	CaCl ₂ and Urea (CO(NH ₂) ₂)

¹Produce exocellular metabolic substances (EPS)

²Produce EPS with non-uerolytic (NU) calcite (CaCO₃)

³Produce EPS with uerolytic (U) calcite (CaCO₃)

3.3 Microbial Growth Medium

DRG3 and RB-05 biomass were produced in the laboratory from nutrient broth (NB)-bacteria incubated culture by centrifuging at 7000 rpm for 10 min at 4°C.

The bacterial growth medium within the sand matrix composed of nutritional minerals: glucose (20 g/L), NH₄Cl (3 g/L), MgSO₄ (0.6 g/L), NaCl (0.14 g/L), ZnSO₄ (2.3mg/L), MnSO₄(17mg/L), CU₂SO₄(10mg/L), Na₂MoO₄ (4 mg/L), EDTA (40 mg/L), NiCl₂ (0.4 mg/L), NaI (6.6 mg/L), KH₂PO₄ (0.14 g/L), K₂HPO₄ (2.2 g/L); reactive minerals: CaCl₂ (0.1 g/L) and CO(NH₂)₂ (3 g/L) based upon the medium characteristics of metabolic pathways of microbes used for this research (Ghatak 2017).

4 EXPERIMENTAL INVESTIGATION

4.1 Measurement of B_w value

A cylindrical sand sample of approximately 38 mm diameter and 76 mm height prepared within a thin latex membrane fixed with cyclic triaxial bottom pedestal using a sterilized cylindrical split mold. Sterilized dry sand of about 133 gm was pluviated under 50 ml elevated nutrient media within the cylindrical mold. For bacteria-inoculated sand samples, an additional 0.3 gm biomass of respective bacterial strain (DRG3 and RB-05) uniformly mixed with this media to hosting live bacterial population within the sand specimen. The height and rate of pluviation were adjusted to achieve a post incubated relative density of about 40±2%. The entire activities were carried out within a laminar airflow chamber to avoid aerobic microbial contamination. The samples were serially incubated from 12 to 72 hours at 35°C under an overlying surcharge of 118 gm to prevent the bulging from biogenic CO₂ gas removal. The overlying surcharge media on the sand sample ensures the fully saturated condition, and it removed before placed in the cyclic triaxial frame.

The incubated sample of each 12 hours interval was removed from the cylindrical mold and placed within the cyclic triaxial cell by fitting the sample axially with top pedestal. The triaxial chamber was then assembled and filled with de-aired water. This entire system then placed in a cyclic triaxial frame supplied by Heico, India, and closed the de-aired water-saturated drainage line. The sample was then subjected to a cell pressure of

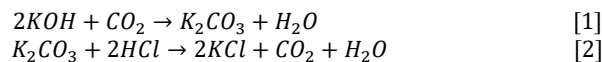
100 kPa through a pneumatic control panel. The corresponding pore pressure was recorded through an attached pore pressure transducer, which was used to evaluate the B_w value of such an incubated sand sample. These activities were carried out for the entire 72 hours of incubated sand samples.

Similar studies were made in a static triaxial sample of approximately 37 mm diameter and 74 mm height with identical characteristics to record the B_w value, which also presented in this paper (Ghatak 2017).

4.2 Measurement of Free and Dissolved CO₂

Aerobic microorganism produces CO₂ from dissolved oxygen of nutrient media. The free CO₂ gas was measured to estimate the degree of unsaturation, and its effects on the compressibility of pore fluid and B_w value. For this, a closed system experimental set up prepared within a UV and formaldehyde sterilized humidity chamber. The dry sterilized sand grains of about 120 gm uniformly distributed by pluviating under 50 ml nutrient media mixed with 0.3 gm respective bacterial strain within a 143 mm Petri dish to ensuring minimum biogas entrapment within the sand specimen. The treated petri dish sample was placed below the perforated plate of a 6L sterilized desiccator. A standard 20 ml 0.5 (N) KOH in a 50 ml sterilized beaker was placed above the perforated plate to entrap the free biogenic CO₂. Three 100 ml respective media within sterilized 200 ml beaker, buffered at pH 6.0, pH 7.0 and pH 8.0 through 0.25 (N) HCl and 1(N) NaOH were placed above the perforated plate at three different desiccators to maintain that certain pH effect on biological activities. A filter cloth was attached with the perforated plate to restrict the bacterial movement above the perforated plate. The identical bacteria-free control petri dish sample was also kept in the desiccator at three different pH levels for atmospheric CO₂ entrapment. An experimental run was carried out without any pH effect to distinguish the pH effects. The desiccators were kept in a darkened humidity chamber to incubate the sample at 35°C temperature, 1 atm pressure, and 60±2% relative humidity for 72 hours. The tests were performed triplicate for each case to show the uniformity of results (ASTM D5988–12). The CO₂ production in triaxial samples is expected to be similar to that produced in Petri plates.

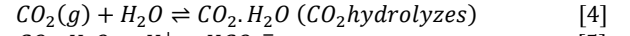
The free CO₂ produced from bacterial activities within the bacteria-inoculated Petri plate sample trapped in 0.5 (N) KOH solutions expressed as $[CO_2]_{KOH}$. Thus KOH solutions were changed at every 12 hours interval for the entire 72 hours incubation period. The amount of trapped CO₂ estimated through titrating that 20 ml KOH solution against 50ml 0.25 (N) HCl in a burette using a 0.5% phenolphthalein indicator solution. The quantity of CO₂ determined stoichiometrically from the amount of 0.25 (N) HCl, which indicates the amount of K₂CO₃ formed due to CO₂ absorption as per Equation 1 and Equation 2.



The actual amount of trapped CO₂ in 0.5 (N) KOH obtained from Equation 3.

$$[CO_2]_{KOH} = [CO_2]_{(Treated)} - [CO_2]_{(Control)} \quad [3]$$

The dissolved carbon dioxide concentration in 100 ml media of three pH levels was calculated from Carbon dioxide-water equilibrium parameters, i.e., pH and corresponding dissolved inorganic carbon (Seinfeld and Pandis 2006), described below (as in Eq. 4-16).



The equilibrium constants for the above reactions at 298°K temperature are expressed in Equation 7-10 accordingly (Seinfeld and Pandis 2006).

$$k_{HC} = H_{CO_2} = \frac{[CO_2 \cdot H_2O]}{p_{CO_2}} \quad [7]$$

Where k_{HC} is the Henry's solubility constant for carbon dioxide = $3.4 \times 10^{-2} \text{ (mol.L}^{-1} \cdot \text{atm}^{-1})$ at 298°K (Ghatak et al. 2017); p_{CO_2} is the partial pressure of CO₂.

$$K_{C1(298)} = \frac{[H^+][HCO_3^-]}{[CO_2 \cdot H_2O]} = 4.3 \times 10^{-7} \text{ mol. atm}^{-1} \quad [8]$$

$$K_{C2(298)} = \frac{[H^+][CO_3^{2-}]}{[HCO_3^-]} = 4.68 \times 10^{-11} \text{ mol. atm}^{-1} \quad [9]$$

The equilibrium constants at temperature T (in °K) are represented by Equation 10.

$$K_{(T)} = K_{(298)} \exp \left[-\frac{\Delta H}{R} \left(\frac{1}{T} - \frac{1}{298} \right) \right] \quad [10]$$

Where, $-\Delta H/R$ (K) = -1000 and -1760 for K_{C1} and K_{C2} respectively.

The total dissolved carbon dioxide $[CO_2^T]$ is given by Equation 11-12.

$$[CO_2^T] = [CO_2 \cdot H_2O] + [HCO_3^-] + [CO_3^{2-}] \quad [11]$$

$$\therefore [CO_2^T] = H_{CO_2} \cdot P_{CO_2} \left[1 + \frac{K_{C1}}{[H^+]} + \frac{K_{C1} \cdot K_{C2}}{[H^+]^2} \right] \quad [12]$$

Where the actual amount of dissolved CO₂ obtained from the following expression (Equation 13):

$$[CO_2^T]_{Actual} = [CO_2^T]_{pH(Treated)} - [CO_2^T]_{pH(Control)} \quad [13]$$

The total dissolved carbon dioxide is expressed by Equation 14.

$$[CO_2^T] = H^*_{CO_2} \cdot p^*_{CO_2} \quad [14]$$

$H^*_{CO_2}$ is defined as effective Henry's law constant for CO₂, which indicates the solubility of CO₂ on the respective pore medium, expressed as $\text{mol.L}^{-1} \cdot \text{atm}^{-1}$.

The effective partial pressure ($p^*_{CO_2}$) of dissolved CO_2 is determined from the following expression (Equation 15).

$$p^*_{CO_2} = \frac{1}{100} \left[\frac{[CO_2]_{KOH} + [CO_2^T]_{Actual}}{Volume\ of\ desiccator\ (ml)} \right] \times p_a \quad [15]$$

The pH of the medium is defined as Equation 16.

$$pH = -\log_{10}[H^+] \quad [16]$$

4.3 Bacterial Growth Strategy

Bacterial population size is an important influencing factor for microbial growth levels and corresponding bio-mineral precipitation and biogenic CO_2 generation. Hydrolyzed CO_2 decreases the pH of the pore fluid, as shown in Figure 1.

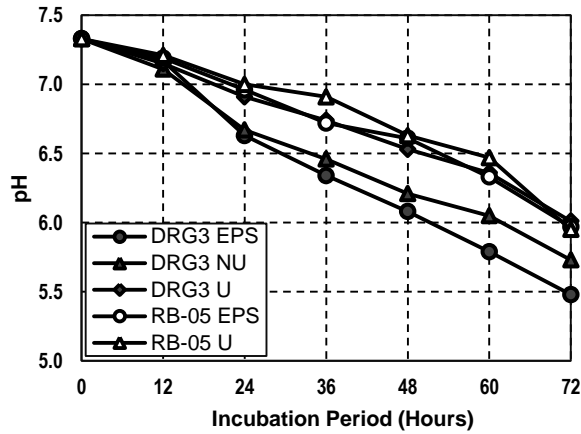


Figure 1. Effect of hydrolyzed biogenic CO_2 on the pH of nutrient pore fluid.

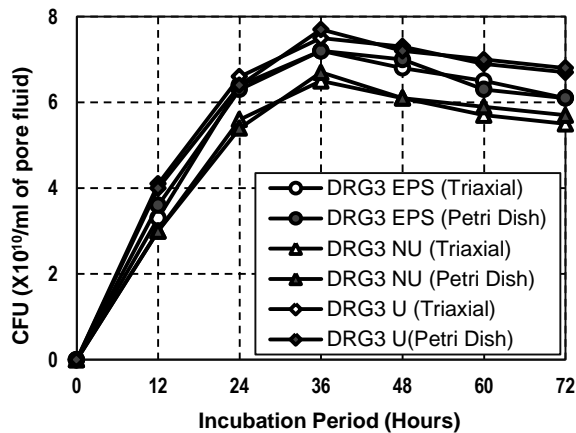


Figure 2. DRG3 population growth within cyclic triaxial and Petri dish samples at three metabolic pathways.

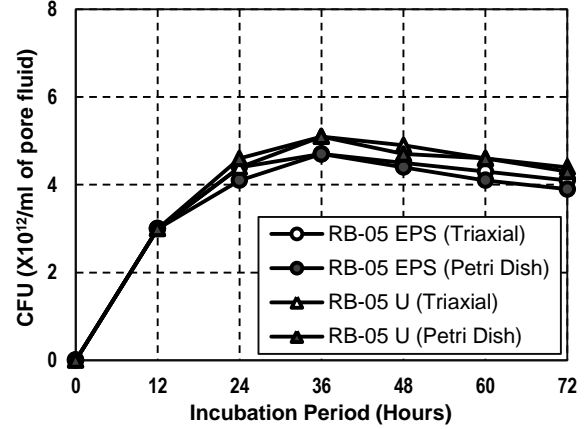


Figure 3. RB-05 population growth within cyclic triaxial and Petri dish samples at three metabolic pathways.

The microbial load level within the sample was expressed in terms of the colony-forming unit (CFU), which follows the same trend with free CO_2 , as shown in Figure 2 and Figure 3.

CFU is estimated by serial dilution spread plate technique (ASTM D5465-16) and expressed corresponding to the volume of pore fluid. The supernatant of bacteria-inoculated pore fluid collected at 12 hours intervals during incubation was serially diluted to 10^{-16} and 0.1 ml of each diluted solution transfer to the solid nutrient agar media plates and incubated at $35^\circ C$ for 12 hours. CFU determined from bacterial colonies on the plate of the corresponding diluted solution that appears within the range of 30 to 300. From the CFU plots in Figure 2 and Figure 3, it is stated that the CO_2 production in triaxial samples is nearly the same as that produced in Petri plates.

5 B_w - VALUE ANALYTICAL MODELLING

For a bacteria-inoculated sand sample, the medium consists of incompressible mineral grains and liquid-gas mixture phase within the pore space. Skempton's (1954) pore pressure parameter (B_w) represents a proportionality constant between isotropic confining pressure on the sample ($\Delta\sigma$) and developed pore pressure (Δu) within the sample (Eq.17) (Ghatak 2017).

$$B_w = \frac{\Delta u}{\Delta\sigma} = \frac{1}{1 + n(K_s/K_f)} \quad [17]$$

Where n is the porosity, K_s is the bulk modulus of incompressible mineral skeleton consist of bio-products (i.e., EPS, Calcite, etc.) within soil matrix and sand grains, and K_f is the bulk modulus of pore fluid.

The solid phase compressibility can be approximated by the following Equation 18.

$$\frac{1}{K_s} = \frac{1}{100} \left[\frac{A}{K_{bs}} + \frac{(100 - A)}{K_{ms}} \right] \quad [18]$$

Where K_{bs} is the bulk modulus of bio-products, K_{ms} is the bulk modulus of mineral grains, and A is the gravimetric percentage of bio-products in terms of the dry weight of soil minerals.

It was observed that the maximum amount of bio-products (about 1.6 gm of EPS and 1 gm of calcite) were minimal compared to the amount of soil mineral grains (120 gm). Therefore, $A \approx 0$. Hence $K_s \approx K_{ms}$.

The compressibility of the sand skeleton for confining pressure about 100 to 200 kPa, $1/K_s$, was about 12 MPa^{-1} (Ghatak et al. 2017). The water vapor effect in the compressibility of soil was neglected due to dependency on relative humidity.

The compressibility of the bacteria-inoculated pore liquid and biogenic gas mixture expressed through Equation 19 (Ghatak et al. 2017).

$$\frac{1}{K_f} = \frac{1}{K_{f1}} + \frac{1}{K_{f2}} \quad [19]$$

Where K_{f1} is the bulk modulus of pore liquid containing dissolved gasses, K_{f2} is the bulk modulus of pore liquid-gas mixture present in void space.

Generally, for aerobic bacterial activities at atmospheric conditions, biogenic gasses O_2 , N_2 , and CO_2 dissolved within the pore liquid and affected the bulk density of the liquid phase as per Equation 20 (Fredlund 1967).

$$K_{f1} = 1/\{S(h_{O_2}/K_{O_2}) + S(h_{N_2}/K_{N_2}) + S(h_{CO_2}/K_{CO_2})\} \quad [20]$$

Where S is the saturation ratio and represents as a function of pore fluid pH, h_{O_2} , h_{N_2} , and h_{CO_2} are the volume fractions of dissolved oxygen, nitrogen and carbon dioxide in void space at a particular temperature and pressure, respectively. K_{O_2} , K_{N_2} , and K_{CO_2} are the bulk modulus of the respective gases.

The bacteria-inoculated samples incubated at constant temperature and pressure (35°C and 1atm); thus, the process is assumed to be isothermal. For such an isothermal process, bulk moduli of the above gas are equal to the applied pressure. Hence the Equation 20 is modified as Equation 21.

$$K_{f1} = 1/\{(Sh_{O_2} + Sh_{N_2} + Sh_{CO_2})/u_w\} \quad [21]$$

The concentration of these gases dissolved in pore fluid, c_a , is governed by Henry's Law (Equation 22).

$$k_H = c_a/p_g \quad [22]$$

Where, k_H is Henry's solubility constant ($\text{mol.L}^{-1}.\text{atm}^{-1}$), and p_g is the partial pressure of these gases.

The temperature dependence of k_H is represented in °K, according to Equation 23.

$$k_{H(T)} = k_{H(T^-)} \exp\{C(1/T - 1/T^-)\} \quad [23]$$

Where $k_{H(T)}$ and $k_{H(T^-)}$ are the values of k_H at a given temperature, T , and at standard temperature, T^- (i.e., 298°K), respectively; and C is a constitutive

constant for a species of gas expressed in °K, listed in Table 2.

Further partial pressure depends on the volume fraction of the gas in the atmosphere, V_p , and atmospheric pressure, p_a (1atm) (Equation 24).

$$p_g = (V_p/100) \times p_a \quad [24]$$

Table 2. Input parameters for B_w value modeling (Ghatak et al. 2017)

Biogenic Gas	$k_{H(T^-)}$ ($\text{mol.L}^{-1}.\text{atm}^{-1}$)	C (°K)	V_p (%)
O_2	1.3×10^{-3}	1700	20.95
N_2	6.1×10^{-4}	1300	78.09
CO_2	3.4×10^{-2}	2400	0.04

The bulk modulus of liquid phase due to occluded bubbles accounted for the bulk moduli of nutrient medium, K_w (which is considered equal with water, ~ 2.2 GPa), and gas bubbles K_b , expressed in Equation 25 (Rebata-Landa and Santamarina, 2012).

$$K_{f2} = 1/\left\{\left(\frac{S}{K_w}\right) + \frac{(1-S)}{K_b}\right\} \quad [25]$$

The bulk modulus of gas bubbles is equal to its internal pressure. The gas bubble internal pressure, P , correlates to the pressure within the void space, u_w by $P = u_w + 2T_s/r$, where T_s is the surface tension of water containing dissolved gases, and r is the bubble radius. According to Rebata-Landa and Santamarina (2012), r , for occluded bubbles, is expected to be as small as ~0.054mm and, therefore $P \approx u_w$. As the free gas present in soils, the effect of capillarity is not considered in this study.

Hence through combining the above equations, the modified expression of Skempton's B_w parameter for bacteria-inoculated sand can be expressed as per Equation 26.

$$B_w = \frac{1}{1 + nK_s/\left\{\frac{S}{K_w} + \frac{(1-S)}{u_w} + \frac{(Sh_{O_2} + Sh_{N_2} + Sh_{CO_2})}{u_w}\right\}} \quad [26]$$

6 EFFECT OF PH ON FREE BIOGENIC CO_2

Hydrolyzed biogenic CO_2 significantly decreases pore fluid pH, which successively affects the production of free CO_2 . To study such effect, the free CO_2 trapped at controlled pH level 6.0, 7.0, and 8.0. It observed from Figure 4-6 that at pH 6.0, dissolved CO_2 quantity is small compared to pH 8.0, so the free CO_2 trapped in KOH at pH 6.0 attains a higher value than pH 7.0 and 8.0 accordingly.

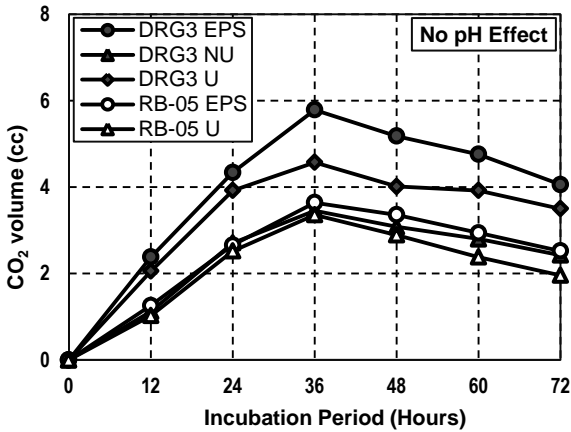


Figure 4. Free biogenic CO₂ trapped in KOH without any pH effects for DRG3 and RB-05 biological activities at metabolic pathways.

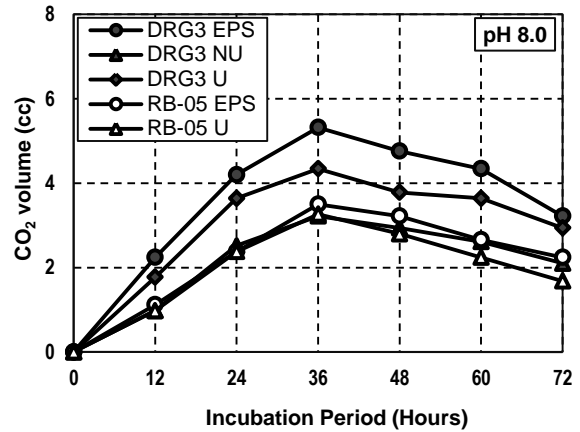


Figure 7. Effect of pH 8.0 on free biogenic CO₂ entrapment in KOH for DRG3 and RB-05 biological activities at metabolic pathways.

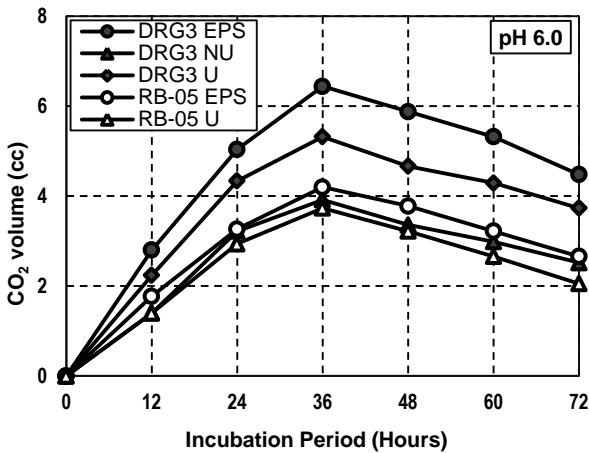


Figure 5. Effect of pH 6.0 on free biogenic CO₂ entrapment in KOH for DRG3 and RB-05 biological activities at metabolic pathways.

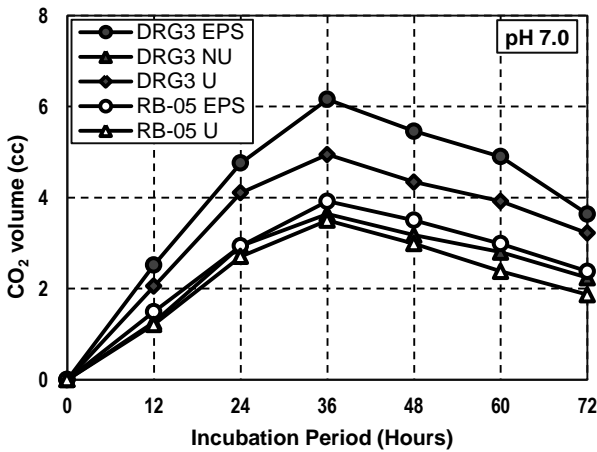


Figure 6. Effect of pH 7.0 on free biogenic CO₂ entrapment in KOH for DRG3 and RB-05 biological activities at metabolic pathways.

7 EFFECT OF PH ON SOLUBILITY OF CO₂

The solubility of biogenic CO₂ on nutrient pore medium of the bacteria-inoculated sand sample determined from aqueous phase chemical equilibrium of that medium. In this study, the solubility of CO₂ determined from the dissolved quantity of CO₂ on the pore fluid at three different pH levels at 35°C and 1 atm pressure. From Figure 8., it is shown that the CO₂ solubility attains a higher value for RB-05 activities within the pore space and has a low value at EPS media under DRG3 biological activities. So it can strongly state that the bio-product on that respective media has a significant effect on solubility, which will be presented in the next investigation.

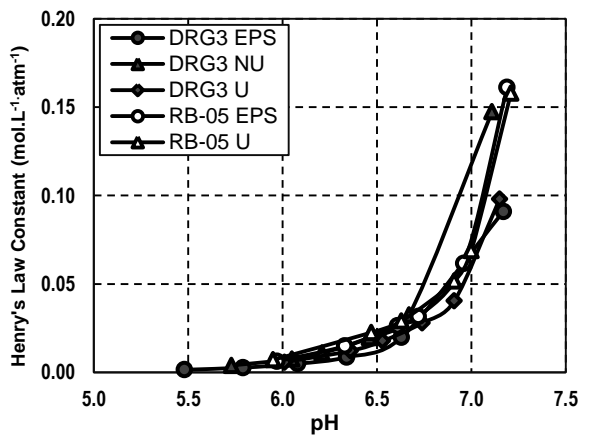


Figure 8. Effect of pore fluid pH on solubility of biogenic CO₂ for DRG3 and RB-05 bacterial activities at three metabolic pathways.

8 EFFECT OF PH ON B_W- VALUE

It has already described that the dissolved and free biogenic CO₂ strongly dependent on the pH of the nutrient pore medium. Dissolved CO₂ expresses the

solubility on that medium. Correspondingly free biogenic CO_2 affects the pore fluid compressibility and B_w value of the bacteria-inoculated sand sample. The results are present graphically, which shows the effect of pH on B_w value with corresponding experimental observation.

For the DRG3 EPS inoculated sand sample, the maximum difference between calculated and experimental B_w value is reduced from 3.12% to 0.20% due to the pH effect of pore fluid (Figure 9).

From Figure 10., it observed that the maximum difference between calculated and experimental B_w value is reduced from 3.12% to 1.99% due to the pH effect of pore fluid of DRG3 NU inoculated sand sample.

For the DRG3 Uerolytic inoculated sand sample, the maximum difference between calculated and experimental B_w value is reduced from 3.72% to 2.42% due to the pH effect of pore fluid (Figure 11).

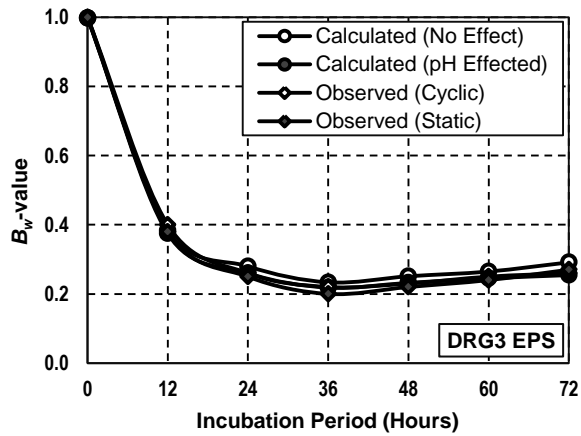


Figure 9. Effect of pore fluid pH on B_w value of DRG3 EPS inoculated sand sample.

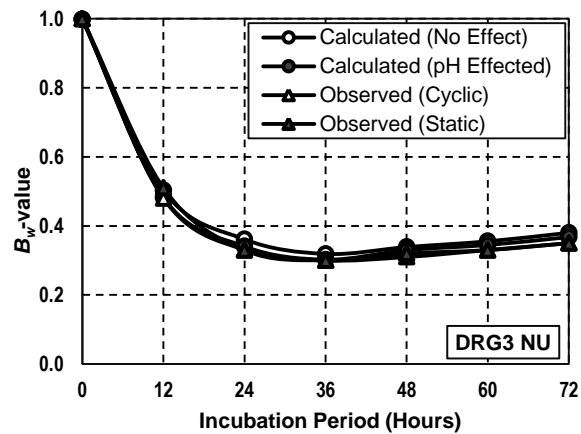


Figure 10. Effect of pore fluid pH on B_w value of DRG3 Non-uerolytic inoculated sand sample.

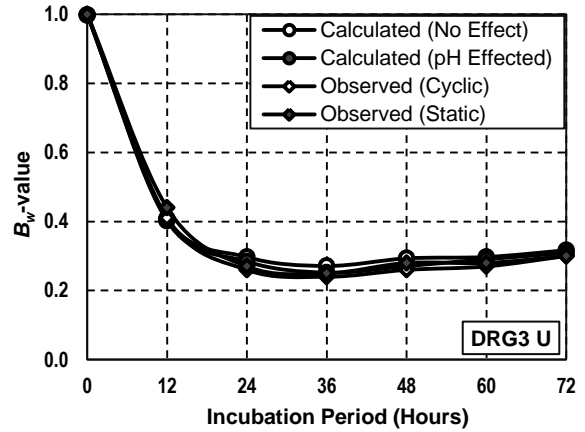


Figure 11. Effect of pore fluid pH on B_w value of DRG3 Uerolytic inoculated sand sample.

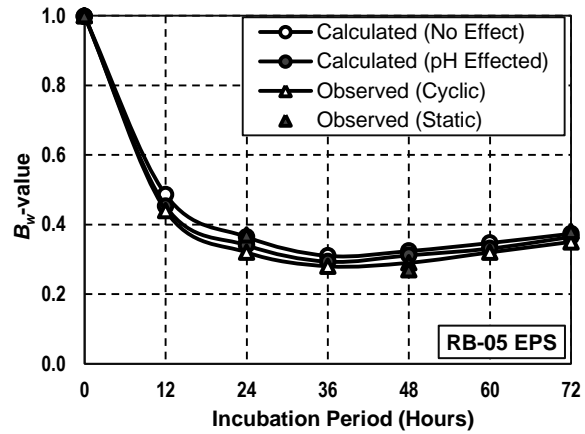


Figure 12. Effect of pore fluid pH on B_w value of RB-05 EPS inoculated sand sample.

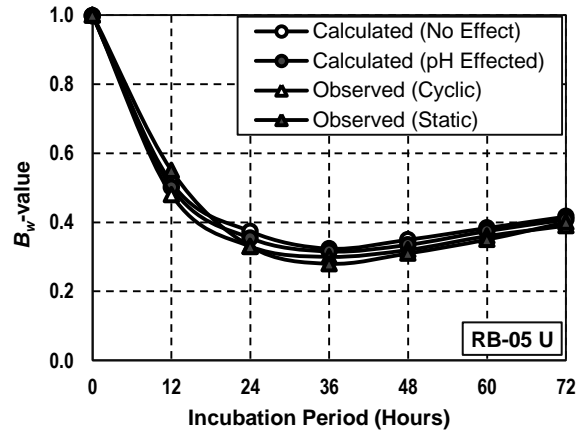


Figure 13. Effect of pore fluid pH on B_w value of RB-05 Uerolytic inoculated sand sample.

For the RB-05 EPS inoculated sand sample, the maximum difference between calculated and

experimental B_w value is reduced from 4.6% to 2.14% due to the pH effect of pore fluid (Figure 12).

From Figure 13., it observed that the maximum difference between calculated and experimental B_w value is reduced from 4.36% to 2.42% due to the pH effect of pore fluid of RB-05 Uerolytic inoculated sand sample.

9 CONCLUSIONS

The conclusions are drawn on the above discussions based on the aim of this study with corresponding results. All the outputs in this investigation were satisfied with repeatability.

From the point of view on biogenic CO_2 effects, the pore fluid pH increase with dissolved CO_2 and the high free CO_2 form at a lower pH level as the solubility will decrease at an acidic pH level of pore fluid.

The high solubility of CO_2 on the RB-05 inoculated media proves that the solubility is also affected by bio-products (i.e., EPS and Calcite) on such media, which provide a unique magnitude of solubility than other media.

From the study of pH effect of pore fluid on B_w value, it has shown that the maximum effect observed at DRG3 EPS inoculated sample, where the observed and calculated B_w value difference reduced by 2.93%, whereas for RB-05 EPS, RB-05 U, DRG3 U, and DRG3 NU exhibit the values of 2.45%, 1.94%, 1.30%, and 1.13%, respectively.

10 REFERENCES

ASTM D5465 – 16. 2012. Standard Practices for Determining Microbial Colony Counts from Water Analyzed by Plating Methods, © ASTM International, West Conshohocked, USA.

ASTM D5988 – 12. 2012. Standard Test Methos for Determining Aerobic Biodegradation of Plastic Materials in Soil, © ASTM International, West Conshohocked, USA.

Cheng, L., Cord-Ruwisch, R. and Shahin, M. A. 2013. Cementation of Sand Soil by Microbially Induced Calcite Precipitation at various degrees of Saturation, *Can. Geotech. J.*, 50(1), 81-90.

Fredlund, D. G. 1976. Density and Compressibility Characteristics of Air-Water Mixtures, *Can. Geotech. J.*, 13, 386-396.

Ghatak, S. 2017. Influence of Bacterial Activities on Deformation Behavior of Sands, PhD thesis, Indian Institute of Technology, Kharagpur, WB 721302, India.

Ghatak, S., Roy, D. and Roy, S. 2017. Effect of Biogenic Gas on Skempton's Pore Pressure Parameter B_w , PanAM Unsaturated Soils 2017, ASCE, 359-369.

Rebata-Landa, V. and Santamarina, J. C. 2012. Mechanical Effects of Biogenic Nitrogen Gas Bubbles in Soils, *J. Geotechnical. Geoenv. Eng.*, ASCE, 138(2), 128-137.

Seinfeld, J. H. and Pandis, S. N. 2006. Atmospheric Chemistry and Physics: From Air Pollution to Climate Change, Second Edition, © Jhon Wiley & Sons, Inc.

Sills, G. C., Wheeler, S. J., Thomas, S. D. and Gardner, T. N. 1991. Behavior of Offshore Soils Containing Gas Bubbles, *Geotechnique*, 41(2), 227-241.

Skempton, A. W. 1954. The Pore-Pressure Coefficients A and B, *Geotechnique*, 4(4), 143-147.